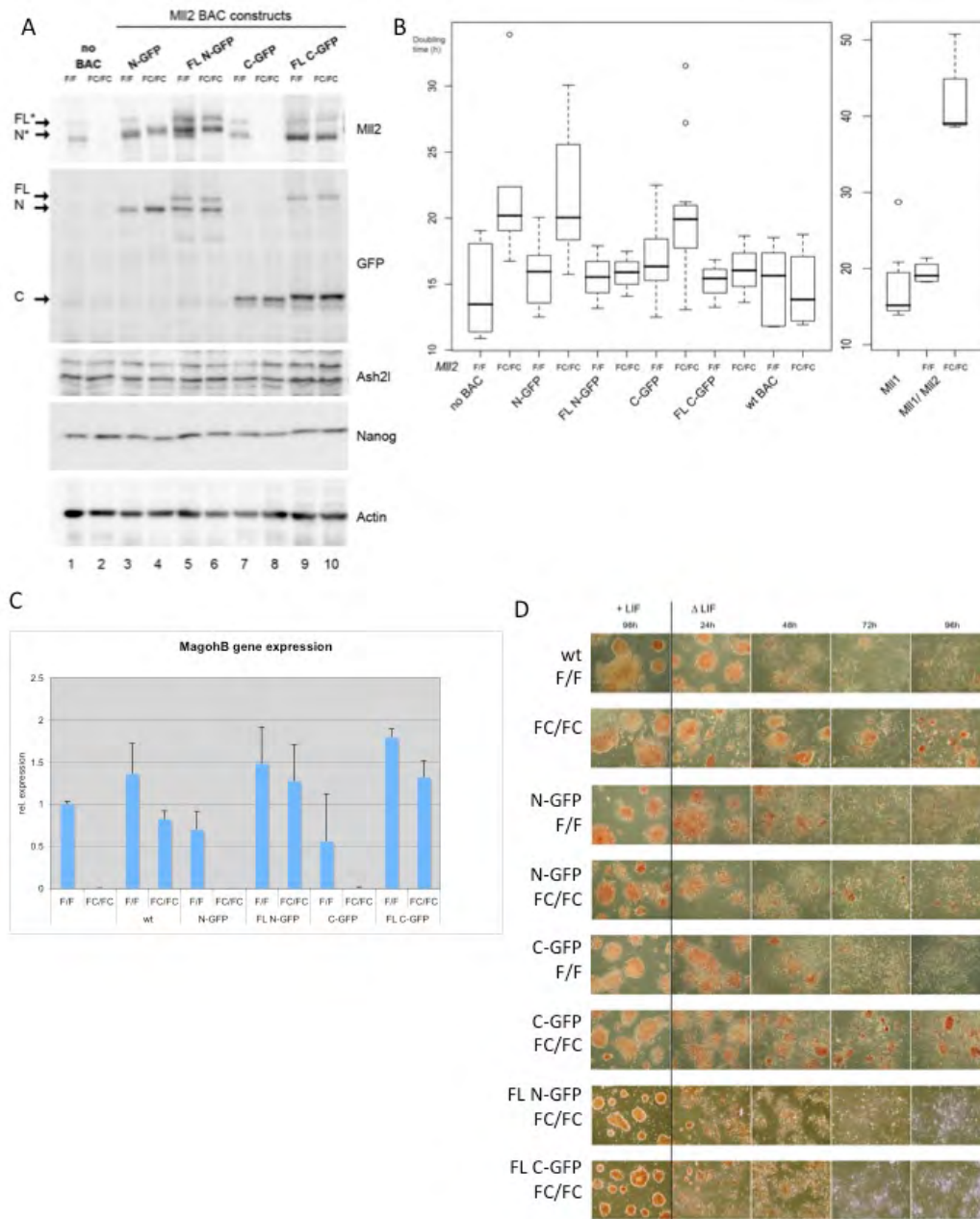


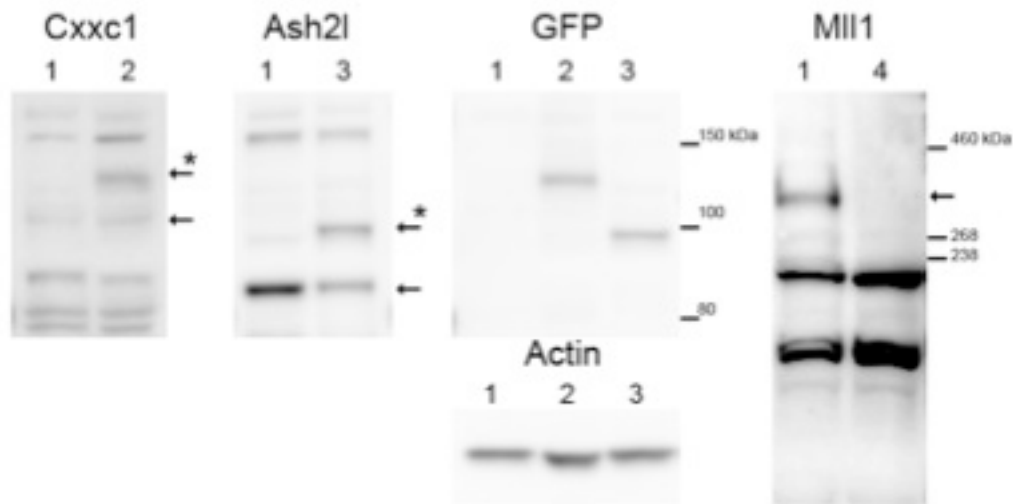
Denissov Suppl. Figure 1

**Supplementary Figure 1. Diagram of the *Mll2* alleles.** At the top the full *Mll2* structural gene is depicted with exons shown in green. By gene targeting, a stop cassette consisting of a splice acceptor, lacZ-neo or lacZ-hygro fusion cassette with poly adenylation signal was introduced into intron 1. It was surrounded by FRT sites (red triangles). The second exon was also flanked by loxP sites (yellow triangles). Targeting both alleles produced *Mll2*<sup>-/-</sup> ESCs because the stop cassette blocks downstream expression (Glaser et al. 2006). FLP recombination (third line) removed the stop cassette restoring wild type function and establishing the *Mll2*<sup>F/F</sup> genotype. Cre recombination, mediated by CreERT2 targeted to the *Rosa26* locus and tamoxifen induction, deletes the second exon provoking a frame shift and the *Mll2*<sup>FC/FC</sup> genotype. Because the exon/intron structures of the two sister genes, *Mll1* and *Mll2*, are virtually identical, the *Mll1* alleles are the same. To make the *Mll1*<sup>-/-</sup> cells, after targeting both alleles the FRT flanked stop cassette was left in and Cre recombinase was used to delete both 2<sup>nd</sup> exons. In the middle, the protein features are illustrated with the key at the bottom. The position of the GFP tags either side of the taspase cleavage sites is indicated and the four different tagged proteins are illustrated.



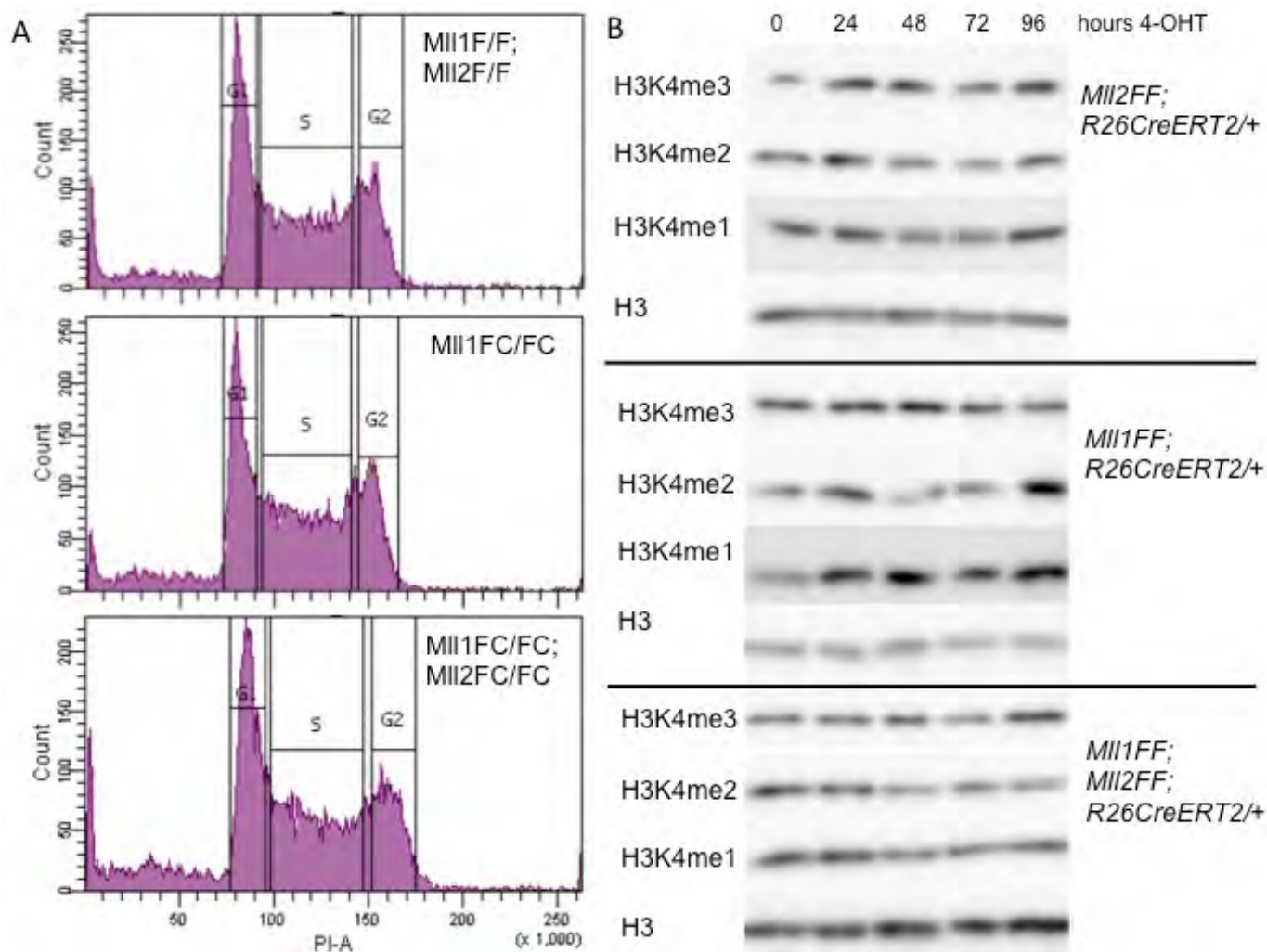
Denissov Suppl. Figure 2

**Supplementary Figure 2. Functional rescue by the tagged MII2 BAC transgenes.** (A) *MIl2*<sup>F/F</sup> cells (lane 1) were lipofected with BAC transgenes expressing either the N-terminus of MII2 until the taspase cleavage site with GFP attached to the C-terminus (N-GFP; lanes 3 and 4); full length MII2 with GFP attached on the N-terminal side of the taspase cleavage site (FL N-GFP; lanes 5 and 6); the C-terminus from the taspase cleavage site with GFP attached to its N-terminus (C-GFP; lanes 7 and 8) or full length MII2 with GFP attached on the C-terminal side of the taspase cleavage site (FL C-GFP; lanes 9 and 10). The cells were induced with 4-hydroxy tamoxifen to eliminate endogenous MII2 expression (lanes 2, 4, 6, 8 and 10) or not (lanes 1, 3, 5, 7 and 9). From top to bottom panels, the antibodies used were raised against MII2, GFP, Ash2l, Nanog and Actin. As evident in lanes 1 and 7, endogenous MII2 is mostly cleaved by taspase in ESCs. The upper band is uncleaved full length MII2, the lower is the N-terminal product after taspase cleavage. The MII2 antibody does not recognize the C-terminal fragment, which can be seen in the GFP panel when the tag is on the C-terminal part. (B) Summary of ESC doubling times before (F/F) and 144 hours after adding tamoxifen (FC/FC) to remove MII2, MII1 or both with and without the BAC transgenes as indicated. (C) Expression of *MagohB* was evaluated by qRT PCR using *Actin* as the reference mRNA. The ESC lines were the same as described above for panel A. (D) As for Supplementary Fig.2A and C except cells were stained for alkaline phosphatase after removal of LIF for the indicated times, or not. F/F – *MIl2*<sup>F/F</sup>; CreERT2 ESCs before tamoxifen induction of Cre recombination to delete MII2 expression; FC/FC – the same cells 96 hours after tamoxifen addition; wt – stable expression of MII2 from a BAC transgene; N-GFP, stable expression of the GFP tagged N-terminus of MII2 up to the taspase cleavage site; FL-N-GFP, stable expression of full length MII2 from a BAC transgene with GFP inserted at the N-terminal side of the taspase cleavage site; C-GFP, stable expression of the GFP tagged C-terminus of MII2 from the taspase cleavage site; FL-C-GFP, stable expression of full length MII2 from a BAC transgene with GFP inserted at the C-terminal side of the taspase cleavage site.



Denissov Suppl. Figure 3

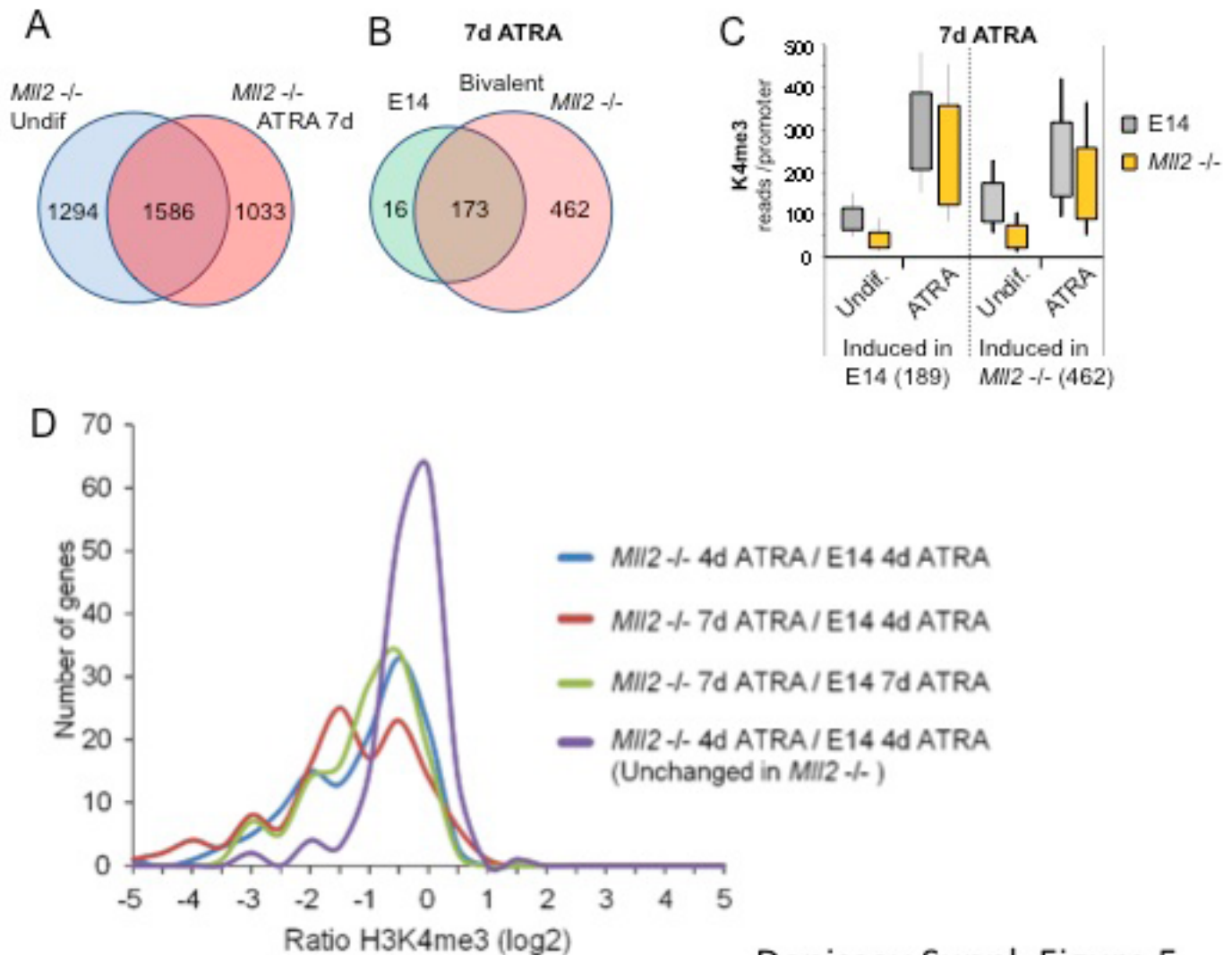
**Supplementary Figure 3. Control western blots.** Western blots were probed with antibodies against the proteins indicated at the top of each panel, which show, from left to right; expression of tagged and endogenous Cxxc1; expression of tagged and endogenous Ash2l; expression of tagged Cxxc1 and Ash2l revealed by an anti-GFP antibody; loss of expressed Mll1 in *Mll1*<sup>-/-</sup> double targeted E14 cells. Lanes 1 – wild type ESCs; lanes 2 – ESCs carrying the Cxxc1 tagged BAC transgene; lanes 3 - ESCs carrying the Ash2l tagged BAC transgene; lane 4 doubly targeted *Mll1*<sup>-/-</sup> ESCs. Arrows denote specific signals; asterisk denotes the tagged proteins.



Denissov Suppl. Figure 4

**Supplementary Figure 4. Further characterization of ESCs lacking Mll1 and Mll2.** (A) FACS sorting of propidium iodine stained cells to evaluate cell cycle distribution. Ablating Mll1 (middle panel) or both Mll1 and Mll2 (lower panel) expression had no effect on cell cycle distribution except for an approximately doubled number of apoptotic events in the absence of Mll2 (Lubitz et al. 2007), revealed here as an increase in stained material to the left of the G1 peak in the lower panel. The double conditional ESC line before tamoxifen-induced recombination served as a control (top panel; *Mll1F/F; Mll2F/F*). (B) H3K4 methylation Western blots of time courses after tamoxifen induction of *Mll1* and *Mll2* mutations. For Mll2 protein, levels are reduced by more than 50% 24 hours after tamoxifen induction and completely gone by 48 hours (Glaser et al. 2009). Overall these results show that neither protein alone or together accounts for bulk H3K4me3.





Denissov Suppl. Figure 5

**Supplementary Figure 5. The promoters that fail to be induced by ATRA in the absence of MII2 do not appear to recover with a longer induction.** Panels A, B and C are equivalent to Figure 4A, B and C except that Figure 4 shows results from 4 days of ATRA induction whereas this figure presents results from 7 days of ATRA induction. (A) After 7 days of ATRA induction, H3K4me3 levels at TSSs were compared between *MII2*<sup>-/-</sup> and E14 ESCs to identify the peaks that were more than 2.5 fold reduced in the absence of MII2 (2619; red circle). These were compared to the 2880 peaks identified in undifferentiated ESCs (Fig. 1A; blue circle). (B) Putative direct bivalent targets of ATRA were identified by comparing H3K4me3 peaks before and after induction. In E14 ESCs, 189 bivalent TSSs (green circle) increased more than 2.5 fold after 7 days ATRA, whereas in *MII2*<sup>-/-</sup> ESCs, most of the same TSSs (173) plus an additional 462 bivalent TSSs (pink circle) increased more than 2.5 fold. (C) Box plot averages of the two categories of bivalent TSSs presented in panel B showed that ATRA induction in both cases resulted in increased H3K4me3 in the absence of MII2. (D) Comparison of H3K4me3 levels between ESCs induced with ATRA for 4 or 7 days revealed that almost all of the promoters impeded at 4 days were still impeded at 7 days, even when compared to the profile in wild type cells after 4 days. A group of 150 genes classified as unaffected were compared between wild type and MII2 mutant ESCs after 4 days ATRA induction to reveal that almost all genes responded in the same way (purple line). In contrast, a group of 150 affected genes showed a bimodal distribution. About half behaved the same in wild type and MII2 mutant ESCs after 4 days of ATRA induction (blue line). The other half was impaired by the absence of MII2. To evaluate whether the impaired promoter response was due to delay, we induced with ATRA for 7 days to observe if the impaired H3K4me3 response was redressed by more time. As shown by comparing either the 7 day mutant to wild type data (green line) or the 7 day mutant to 4 day wild type data (red line), the promoters that were impeded in their response to ATRA remained impeded.